ACERP: Vol. 3, No. 2, (Spiring 2017) 38-44

Advanced Ceramics Progress

Research Article

Journal Homepage: www.acerp.ir

Nanowires Fine Tunable Fabrication by Varying the Concentration Ratios, the Etchant and the Plating Spices in Metal-Assisted Chemical Etching of <111> Silicon Wafer

M. Shavandi[a], A. Massoudi[a*], A. Khanlarkhani[b], M. Moradi[a]

[a]*Department of Semiconductor, Materials and Energy Research Center, Karaj, Iran.*
[b]*Department of Nanotechnology and Advanced Materials, Materials and Energy Research Center, Karaj, Iran.*

PAPER INFO

Paper history:
Received 23 April 2017
Accepted in revised form 11 July 2017

Keywords:
Metal-assisted chemical etching
Silicon nanowires
Etching rate
Concentration ratios

ABSTRACT

The metal-assisted chemical etching (MACE) was used to synthesize silicon nanowires. The effects of etchant concentration, etching and chemical plating time and doping density on silicon nanowires length were investigated. It is shown that increasing the HF and H_2O_2 concentrations leads to etching rate increment and formation of wire-like structure. The results show that the appropriate ratio of concentration to form the silicon nanowires (SiNWs) follows the $[HF]/[H_2O_2]= R$ equation with R values being 2.5, 3 and 3.5, and any deviation from these ratios, results in destruction of wire-like structure. Moreover, the critical etching rates to form the SiNWs are in the range of 4nm/s to 5nm/s. must be Times New Roman 8.

1. INTRODUCTION

Recent years, silicon nanostructures have been considered due to the development of nanotechnology and achieving better properties in wide band gap and increasing the surface to volume ratio in comparison to bulk materials and microstructures. Silicon nanostructures including zero-dimensional, one-dimensional, two-dimensional and three-dimensional nanostructures have also been used in some new devices such as sensors [1], solar cells [2] and lithium-ion batteries [3-5] because of their unique features.

Recent years, silicon nanowires have been identified as one of the well-known 1D nanostructures in many application such as sensors, photonic, photovoltaic and energy storage [6-10]. On the other hand, silicon nanowires have been extensively considered due to their properties that can be changed by length, diameter and direction.

From the past year up to now, silicon nanowires could be synthesized by some methods such as chemical vapor deposition [11], laser ablation [12] and molecular beam lithography [13] which require to use the eutectic temperature of catalyst, vacuum and control of temperature and pressure indicating that there are some challenges in their applications. Moreover, the high cost of process is one of the disadvantages which prevents from commercialization.

Recently, chemical synthesis of SiNWs has been utilized as a simple, efficient and low cost method. Among the chemical methods, metal-assisted chemical etching (MACE) has been introduced as one of the best-known and new methods due to its striking features such as low cost, controllability, fast synthesis and repeatability [14]. In this method, a catalyst is usually utilized to accelerate the process. The basic issue in MACE is explained by the mechanism that is based on holes injection and charge transfer on series of redox reaction at silicon-catalyst interface. On the other hand, the charge transfer plays a key role in MACE [15]. According to this issue, the catalyst is chosen as a noble metal that is deposited on silicon surface and should possess three properties. Some of metals such as Au [16], Ga [17] and Ni [18] have been used as catalyst and each of them shows specific properties forms different structures.

The synthesis of SiNWs by MACE was classified into two categories: one-step synthesis and two-step synthesis. In one-step synthesis, the solvent mixture of noble metal, oxidant which is more electronegative than the silicon agent is generally used [19]. Whereas, in two-step synthesis, two separated solutions are used. In

*Corresponding Author's Email: massoudi.a@gmail.com (A. Massoudi)

this case, the noble metals are initially deposited on silicon surface by one of the
common methods such as sputtering [20], electron beam evaporation [21] and chemical plating [22] and at second step, the samples are immersed in etchant of HF and H_2O_2. On the other hand, for better controlling the parameters and surface structures, two-step synthesis is utilized. The main issue in synthesis of SiNWs is uniform and dense deposition of silver particles layer on silicon surface.
Among the silver deposition methods, silver chemical plating has been widely considered. It appropriates some specific benefits such as cost, controllability and film thickness. The approach is chemical plating of silver particles on silicon surface at the first step. Secondly, chemical etching is applied on silicon wafer which immersed in the etchant of HF and H_2O_2.

First step: Silver particles as a catalyst are deposited on silicon surface [15] due to its potential which leads to injection of the holes to the silicon valence band. Then, silicon surface is oxidized by the holes injection and silver ions are reduced and deposited on silicon surface. Silicon is dissolved by fluorine ions which are available in solution and the silver particles are sunk on silicon surface. In MACE, anodic reaction to reduce the silver ions and cathodic reaction to oxidize the silicon surface are as follows [10]:

$$Ag^+ + e^- \rightarrow Ag \qquad E_0 = +0.79\ V/SHE \tag{1}$$

$$Si + 2H_2O \rightarrow SiO_2 + 4H^+ + 4e^- E_0 = -0.84V/SHE \tag{2}$$

$$Si + 2H_2O + 4h^+ \rightarrow SiO_2 + 4H^+ \tag{3}$$

In the following, silicon is dissolved by fluorine ion according to Eq. (4):

$$SiO_2 + 6HF \rightarrow H_2SiF_6 + 2H_2O \tag{4}$$

Second step: The silicon wafer with silver layer is immersed in mixed etchants of HF and H_2O_2. H_2O_2 is reduced at electrolyte/silver interface [10] according to Eq. 5 and generates holes. The holes transitions from H_2O_2 are accelerated by silver particles. On the other hand, the holes diffuse through silver and then are injected to silver-silicon interface. The holes at interface of silicon and silver particles are considerably more effective than off-metal regions. Then, silicon is etched at regions around the sunken metal particles in silicon.

$$H_2O_2 + 2H^+ \xrightarrow{Ag} 2H_2O + 2h^+ \tag{5}$$

At the second step, silver particles just play an important role as a catalyst to transit holes which is due to H_2O_2 reaction. The other role of silver particles is that they provide a pattern to form the silicon wire-like structures.
Two regimes are considered for anodic reduction: Regime 1 (the tetravalent dissolution) represents sinking process. The regime shows two state of dissolving the silicon. State A is direct dissolution of tetravalent state and state B is dissolution of silicon oxide.
State A:

$$Si + 4h^+ + 4HF \rightarrow SiF_4 + 4H^+ \tag{6}$$

$$SiF_4 + 2HF \rightarrow H_2SiF_6 \tag{7}$$

State B:

$$Si + 2H_2O + 4h^+ \rightarrow SiO_2 + 4H^+ \tag{8}$$

$$SiO_2 + 6HF \rightarrow H_2SiF_6 + 2H_2O \tag{9}$$

In regime 2, divalent dissolution is manifested underneath the silver particles according to Eq. (10):

$$Si + 4HF_2^- + 2h^+ \rightarrow SiF_6^{2-} + 2HF + H_2\uparrow \tag{10}$$

At the end of the processes, this layer is eliminated through Eq. (11). The reaction of nitric acid with silver is terminated by $AgNO_3$ in solution.

$$3Ag + 4\ HNO_3 \rightarrow 3AgNO_3 + NO + 2H_2O \tag{11}$$

There are many principal factors in MACE to form the SiNWs. In order to investigate the etching rate and SiNWs formation, we examined the effect of five factors that have important roles in silicon etching. These five factors are HF concentration, H_2O_2 concentration, chemical plating time, etching time, and doping density of silicon wafer. Therefore, the results are divided into five parts. The purpose of this study is to reveal the variations of etching rate as a function of holes consumption factor (HF), holes generated factor (H_2O_2), processes time and doping density of silicon wafer.

2. EXPERIMENTAL

2.1. Materials The chemical materials are HF (38-40% -Merck), H_2O_2 (30%-Merck) and $AgNO_3$ (99% - Merck). Also, for incipient cleaning, H_2SO_4 (96%-Merck) was used. The silicon wafer (p-type, with crystal orientation of <111> and resistivity of 8-12 Ω.cm) was used and cut to 1*1 cm^2 square. Finally, to remove silver particles layer from surface, HNO_3 (65% - Merck) was used.

2.2. Preparation of sample The silicon wafer (p-type, 8-12 Ω.cm and <111> direction) was cut to 1*1 cm^2 square and washed with acetone and deionize water and immersed into solution of H_2SO_4:H_2O_2 in ratio of 3:1 (v: v) for 10 minutes at room temperature. In this state, the silicon surface was cleaned of organics and a thin oxide layer was formed on surface. In following, the sample was immersed into solution of 5% HF for 3 minutes at room temperature to form the H-terminated on silicon surface and to dissolve oxide layer and prepare the sample for silver deposition.

2.3. Silver particles deposition and Nanowires formation In silver deposition step, the solution including mixture of HF and $AgNO_3$ was treated. Therefore, two solutions with HF concentration of 1.2 M and 4.8 M were prepared for samples 1 and 2, respectively (details are given in Table 1). The concentration of $AgNO_3$ was kept fixed at =0.005 M for all solutions. The samples were placed in these solutions under different times while the solutions were stirred slowly. The process was done at room temperature and room light. In this step, after silver deposition, the samples were become golden yellowish. After the silver was deposited on silicon wafer, the sample was immersed in etchant solution including mixture of HF and H_2O_2 for 30 and 5 minutes in the dark at room temperature according to tables 1 and 2.

TABLE 1. Concentration of etchant for samples 1 and 2, chemical plating time=60 seconds and etching time=30 minutes.

Samples	Sample 1	Sample 2
HF	1.2 M	4.8 M
H_2O_2	0.05 M	0.6 M

TABLE 2. Etchant concentration of eleven samples with etching time=30 minutes and [HF] =4.8 M.

Samples	Sample3	Sample4	Sample5	Sample6	Sample7
[H_2O_2]: [HF](v :v)	1:3.5	1:3.5	1:3	1:3	1:2.5
Chemical plating time	60 Seconds	120 Seconds	60 Seconds	120 Seconds	60 Seconds
Sample8	**Sample9**	**Sample10**	**Sample11**	**Sample12**	**Sample13**
1:2.5	1:5	1:4	1:2	1:1	2:1
120 Seconds	60 Seconds	60 Seconds	60 Seconds	60 Seconds	60 Seconds

2.4. Elimination of silver nanoparticles
For elimination of silver nanoparticles, the sample was immersed in solution mixture of HNO_3: H_2O by ratio of (1:1, v: v) to dissolved the Ag particles, then it was washed by deionize water and was dried by N_2. To remove the oxide layer, the sample was washed with 5% HF and the sample was washed by deionize water and was dried again.

2.5. Characterization The etched silicones surfaces were characterized by X-ray diffraction (Philips- PW3710) in 2θ range from 20 to 70° with Cu-Kα radiation (λ = 1.54056 Å). Morphology of the samples were characterized by FE-SEM (MIRA3 TESCAN) equipped with EDS.

TABLE 3. Three different samples with different H2O2 concentrations, [HF] =4.8 M.

Samples	Sample 3	Sample 5	Sample 7
H_2O_2:HF v:v	1:2.5	1:3	1:3.5

TABLE 4. Different chemical plating times with etchant concentration.

Samples	Sample 5	Sample 6
Chemical plating time	60 seconds	120 seconds
H_2O_2:HF v:v	1:3	1:3

TABLE 5. Different etching times with etchant concentration.

Samples	Sample 3	Sample 9
Etching time	30 minutes	5 minutes
H_2O_2:HF v:v	1:3.5	1:3.5

3. RESULT AND DISCUSSION

Figure 1. shows the FE-SEM cross section image of eight different [H_2O_2]: [HF] ratios. According to Figure 1, formation of structures depends on the concentration ratio of HF and H_2O_2. The HF and the H_2O_2 are used as holes consumption factor and holes generation factor, respectively. Therefore, critical concentrations of HF and H_2O_2 are the main factors to form the suitable structure. On the other hand, four regimes are generally defined to form the structure according to ρ=[HF]/([HF]+[H_2O_2]). In order to consider the silicon etching rate, the comparison of parametric regions of this formula was experimentally investigated as follows: Regime 1, 90% < ρ < 100%: In this regime HF concentration is high and leads to consumption of holes in silicon-metal (silver) interface. As a result, the etching rate of surface depends on H_2O_2 concentration. Figure 3-b shows the etching rate which is decreased to 4 nm/s. This is due to low amount of generated holes in silver silicon interface. Figures 1-a and 1-b show the

FE-SEM cross section images of ρ=92 % and ρ = 90%, respectively.

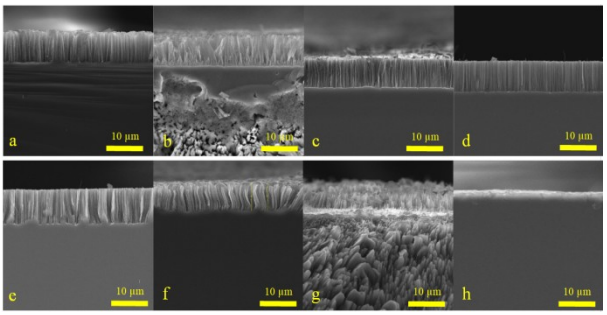

Figure 1. FE-SEM images of a) H_2O_2: HF ratio of 1:5 v: v, b) H_2O_2:HF ratio of 1:4 v: v, c) H_2O_2:HF ratio of 1:3.5 v:v, d) H_2O_2:HF ratio of 1:3 v:v, e) H_2O_2:HF ratio of 1:2.5 v:v, f) H_2O_2:HF ratio of 1:2 v:v, g) H_2O_2:HF ratio of 1:1 v:v, h) H_2O_2:HF ratio of 2:1 v: v.

Regime 2, 85% < ρ < 90%: In this regime some of the injected holes are consumed in silicon-metal (silver) interface. Therefore, SiNWs are generally formed with high porosity. Moreover, some of the holes could not be consumed and the silver particles were re-deposited on SiNWs walls which lead to formation of porous SiNWs. In this regime, the etching rate is increased from 4 to 5.5 nm/s as shown in Figures 3-b. Figures. 1-c, 1-d and 1-e show ρ =89%, ρ =88% and ρ =85%, respectively. As shown in Figures 2 and 3-b, the SiNWs can be formed in this regime.

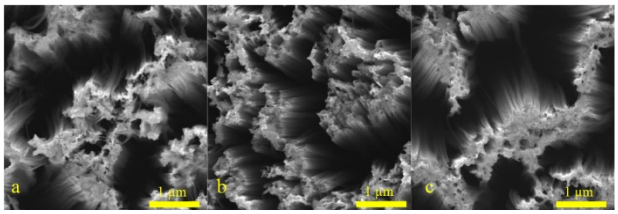

Figure 1. FE-SEM images of a) H_2O_2:HF ratio of 1:2.5 v:v b) H_2O_2:HF ratio of 1:3 v:v, and c) H_2O_2:HF ratio of 1:3.5 v:v.

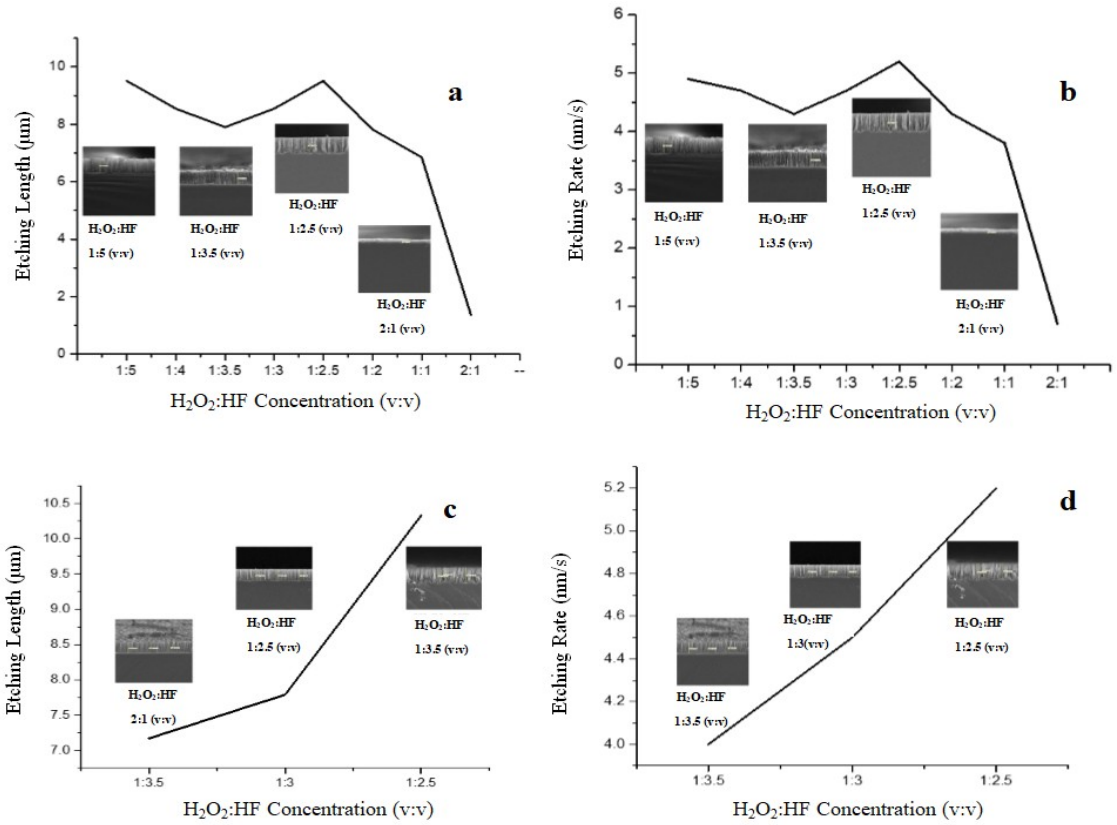

Figure 2. The Graph of p-type silicon wafer <111> wire etching rate and etching length in 4.8M HF concentration, a) Etching length versus concentration for 1 min chemical plating time, b) Etching rate versus concentration for 1 min chemical plating time, c)Etching length versus concentration for 2 min chemical plating time, d) Etching rate versus concentration for 2 min chemical plating time.

3.1. The effect of HF concentration

Figures 4-a and 4-b show the FE-SEM images of silicon wafer <111> in two different HF concentrations of 1.2 M and 4.8M, respectively. As shown in Figure 4, increasing the HF concentration leads to higher etching length.

As Figure 4-c shows, the SiNWs array can be formed with the diameter lower than 100 nm from silicon wafer <111> in 4.8 M HF concentration. Moreover, as can be seen in Figure 4-d, the needle structures are generally observed with diameter of 300 nm up to several µm. On the other hand, the main condition to synthesize SiNWs array with diameters lower than 100 nm is 4.8 M HF concentration.

As the Figure 5-a shows, the etching length for [HF] =1.2 M is significantly is lower than that of the [HF] =4.8 M. According to Figure 5-b, the etching rate at the [HF] =1.2 M and [HF] =4.8 M was 0.7 nm/s and 4.9 nm/s, respectively.

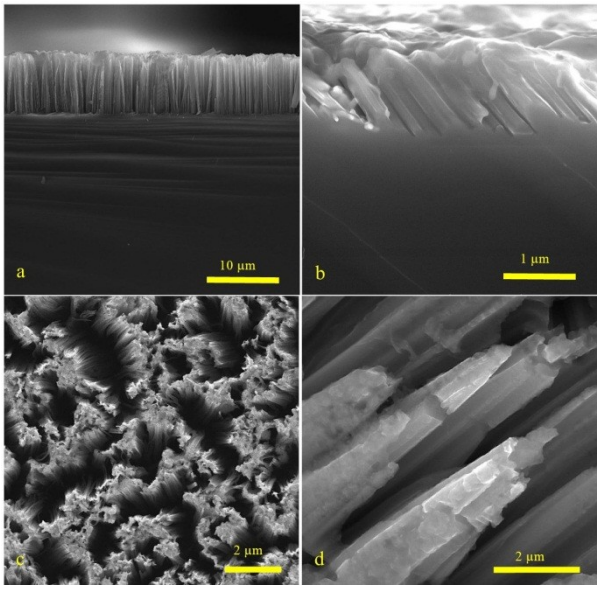

Figure 4. FE-SEM images of silicon etching a and c, [HF]= 4.8 M, and b and d, [HF] =1.2.

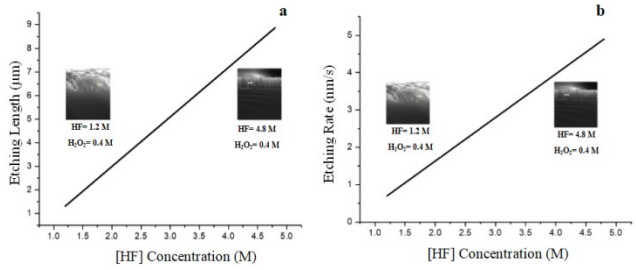

Figure 3. Graph of p-type silicon wafer <111> wire etching in different HF concentration, a) Etching length versus HF concentration, and b) Etching rate versus HF concentration.

3.2. The effect of H_2O_2 concentration

As shown in Figures 1-c, 1-d and 1-e, it is investigated that the SiNWs are formed in the range of $[H_2O_2]$:[HF] 1:2.5 to 1:3.5 (v:v) ratios, respectively. Moreover, as illustrated in Figures 1-a, 1-b, 1-f, 1-g and 1-h, the other structure can be formed by utilizing different H_2O_2 concentration.

As discussed previously, H_2O_2 was used as generator of holes on silicon-metal interface. H_2O_2 was reduced under the silver particles and generates holes in silicon-silver interface. Table 3 shows details of three solutions with different H_2O_2 concentrations to investigate the H_2O_2 concentration effect on the silicon etching. Figure 6 shows the decreasing trend of SiNWs length as the H_2O_2 concentration was decreased, because higher concentration of H_2O_2 increases the holes around silver particles. As a result, the rate of reduction and oxidation are important for forming the SiNWs and other structures. Consequently, it was found that the etching rate can be varied by different H_2O_2 concentrations to form the SiNWs (Figure 1a-h). Figure 3-a shows the etching length curve of these eight samples. The etching length can be in the range of 1 to 10 µm. As can be seen in Figure 3-b, the critical etching rate to form the SiNWs is in the range of 4 to 5 nm/s. Therefore, the best regime to synthesize the SiNWs array is 85-90%.

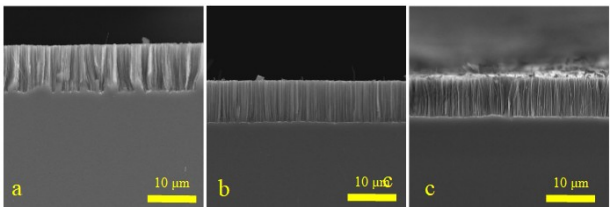

Figure 4. FE-SEM images of a) H_2O_2:HF ratio of 1:2.5 v:v, b) H_2O_2:HF ratio of 1:3 v:v, and c) H_2O_2:HF ratio of 1:3.5 v:v.

3.3. The effect of chemical plating time

Figure 7 shows that the silicon etching length is higher than the etching length when the chemical plating time is 60 seconds. The silver particles are deposited on silicon surface by reduction of silver ions (see also Figure 8-b). As shown in Figure 8, the reduction of Ag^+ occurs and elementary silver is deposited on surface from solution containing HF and $AgNO_3$. Then the localized etching is initiated at particles locations. The silicon oxidation is more around silver particles because of the holes beneath the silver particles are more than the off-metal region. On the other hand, the holes have an important role in MACE, and the alternative redox reaction of Ag^+ leads to injection of holes to silicon bands. The SiNWs array can be formed as a uniform layer via silver deposition on silicon surface. Table 4 shows different chemical plating times for four samples and the results are displayed in Figure 7.

As shown in Figure 3-d, the silicon etching rate for 120 seconds chemical plating is lower than 60 seconds chemical plating. The high etching rate occurs at 60 seconds chemical plating time which is due to low holes consumption rate. This phenomenon traces back to incomplete bonds between fluorine ions and oxidized silicon on the surface of wafer when the chemical plating time is more than 120 seconds. Figure 8 illustrates the MACE mechanism mentioned above

which implies that silver particles sink the silicon surface and lead to formation of SiNWs array. The role of holes transition demonstrates that any linking between silicon and silver particles is not necessary for etching process but the linking is crucial as a pattern for SiNWs formation.

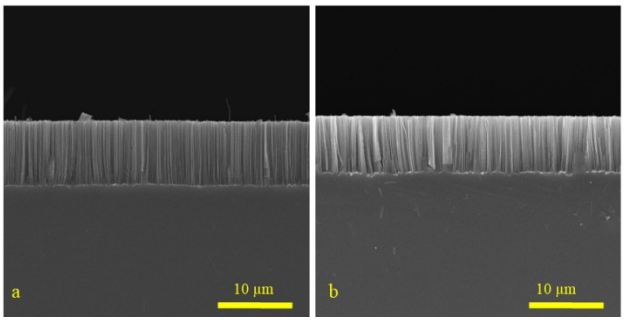

Figure 5. FE-SEM images of a) H_2O_2:HF ratio of 1:2.5 v:v, b) H_2O_2:HF ratio of 1:3 v:v, and c) H_2O_2:HF ratio of 1:3.5 v:v.

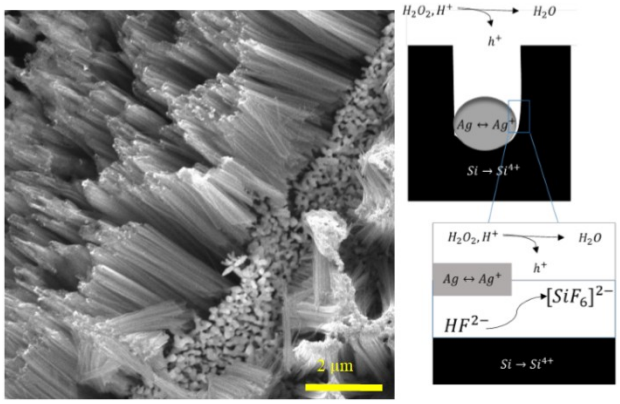

Figure 6. FE-SEM image of SiNWs formation in H_2O_2:HF 1:3 v:v concentration ratio, the silver particles sink silicon surface and SiNWs was formed.

3.4. The effect of etching time

Figure 9, shows the FE-SEM images of the samples prepared by different etching times according to Table 5. Therefore the etching length was increased by varying the etching duration from 5to 30 min.

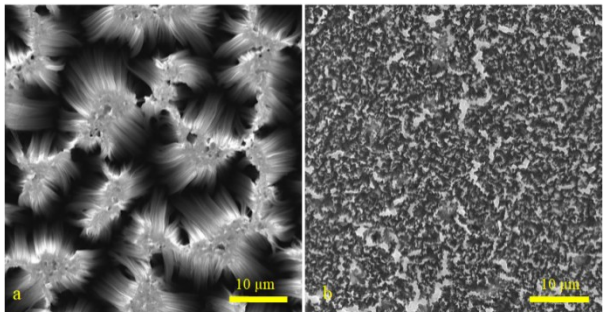

Figure 7. FE-SEM images with H_2O_2: HF ratio of 1:3.5 v:v, a) 5 minutes etching time, b) 30 minutes etching time.

Length of the formed pits was increased by continuous redox couple reaction of silver accompanied by holes transportation. On the other hand, when the etching time is raised, there would be enough time to repeat the cyclic redox reaction and silver particles can sink further. As a result, the silicon is etched at specified rate for different concentrations.

3.5. The effect of doping density of silicon wafer

Figure 10 shows the FE-SEM images of two different samples with different doping density of silicon wafer. Each of doping density forms variety of structures in silicon chemical etching. However as shown in Figure 10, etching rate for p-type 0.005 Ω.cm is faster than p-type 8-12 Ω.cm (Figure 9). On the other hand, holes injection was favored in highly doped (0.005 Ω.cm) Silicon due to less band bending at the highly doped Silicon/electrolyte interface compared to the lightly doped Si. Therefore, the etching rate is high for heavily doped Si rather than the lightly doped Silicon wafer.

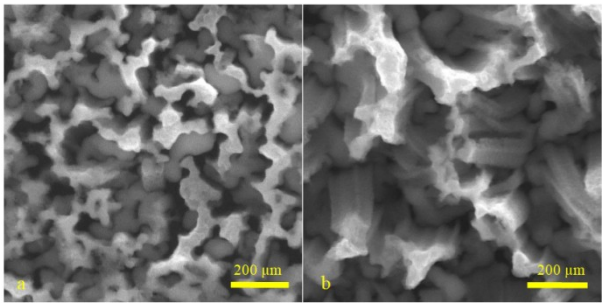

Figure 8. FE-SEM images with H_2O_2:HF 1:3.5 v:v and 5 minutes etching time of a*)* p-type 8-12 Ω.cm, and b*)* p-type 0.005 Ω.cm.

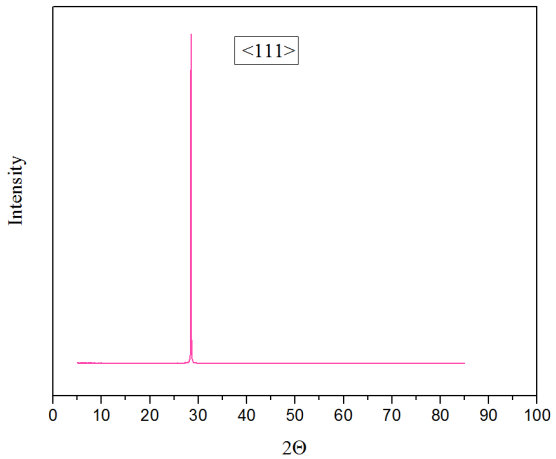

Figure 9. XRD pattern of silicon nanowires synthesis by MACE.

4. CONCLUSION

In summary, synthesis of SiNWs array on silicon wafer <111> (p-type, 8-12 Ω.cm resistivity) was investigated

by MACE in different solutions and different process times. The study of FE-SEM images of silicon top and cross section views explain the relevance ρ=[HF]/([HF]+[H_2O_2]) between holes consumption factor and holes generation factor. The variation of silicon surface etching is strongly function of etchant concentration, process time and doping density of silicon wafer (resistivity) because of the chemical etching mechanism that is based on holes injection and charge transport. As observed, the SiNWs aligned with <111> direction were prepared in the range of ρ=85-90%. On the other hand, the critical concentration ratio to achieve the SiNWs array was [H_2O_2]: [HF] = 1:2.5 to 1:3.5 (v:v). It means that the critical etching rate is 4-5 nm/s.

5-ACKNOWLEDGMENTS

We thank materials and energy research center for supporting this paper.

REFERENCES

1. Li, Z., Chen, Y., Li, X., Kamins, T.I., Nauka, K. and Williams, R.S., "Sequence-specific label-free DNA sensors based on silicon nanowires", ***Nano Letters,*** Vol. 4, No. 2, (2004), 245-247.
2. Kelzenberg, M.D., Turner-Evans, D.B., Kayes, B.M., Filler, M.A., Putnam, M.C., Lewis, N.S. andAtwater, H.A., "Photovoltaic measurements in single-nanowire silicon solar cells", ***Nano letters,*** Vol. 8, No. 2, (2008), 710-714.
3. Wu, H. and Cui, Y., "Designing nanostructured Si anodes for high energy lithium ion batteries", ***Nano Today,*** Vol. 7, No. 5, (2012), 414-429.
4. Massoudi, A., Azim-Araghi, M. and Asl, M.K., " Fabrication of p-Type Nano-porous Silicon Prepared by Electrochemical Etching Technique in HF-Ethanol and HF-Ethanol-H2O Solutions", ***Advanced Ceramics Progress,*** Vol. 1, No. 2, (2015), 24-28
5. Su, X., Wu, Q., Li, J., Xiao, X., Lott, A., Lu, W., Sheldon, B.W. and Wu, J., "Silicon-based nanomaterials for lithium-ion batteries: a review", ***Advanced Energy Materials,*** Vol. 4, No. 1, (2014), 1-7.
6. Tian, B., Zheng, X., Kempa, T.J., Fang, Y., Yu, N., Yu, G., Huang, J. and Lieber, C.M., "Coaxial silicon nanowires as solar cells and nanoelectronic power sources", ***Nature,*** Vol. 449, (2007), 885-889.
7. Chan, C.K., Peng, H., Liu, G., McIlwrath, K., Zhang, X.F., Huggins , R.A. and Cui, Y., "High-performance lithium battery anodes using silicon nanowires", ***Nature Nanotechnology,*** Vol. 3, No. 1, (2008), 31-35.
8. Hochbaum, A.I., Chen, R., Delgado, R.D., Liang, W., Garnett, E.C., Najarian, M., Majumdar, A. and Yang, P., "Enhanced thermoelectric performance of rough silicon nanowires", ***Nature,*** Vol. 451, (2008), 163-167.
9. Laer, R.V., Kuyken, B., Thourhout, D.V. and Baets, R., "Interaction between light and highly confined hypersound in a silicon photonic nanowire", ***Nature Photonics,*** Vol. 9, No. 3, (2015), 199-203.
10. Dubal, D.P., Aradilla, D., Bidan, G., Gentile, P., Schubert, T.J.S., Wimberg, J., Sadki, S. and Romero, P.G., "3D hierarchical assembly of ultrathin MnO2 nanoflakes on silicon nanowires for high performance micro-supercapacitors in Li-doped ionic liquid", ***Scientific Reports,*** Vol. 5, (2015), 9771.
11. Hochbaum, A.I., Fan, R., He, R. and Yang, P., "Controlled growth of Si nanowire arrays for device integration", ***Nano letters,*** Vol. 5, No. 3, (2005), 457-460.
12. Tang, Y.H, Zhang, Y.F., Wang, N., Lee, C.S., Han, X.D., Bello, I. and Lee, S.T., "Morphology of Si nanowires synthesized by high-temperature laser ablation", ***Journal of Applied Physics,*** Vol. 85, No. 11, (1999), 7981-7983.
13. Juhasz, R., Elfström, N. and Linnros, J., "Controlled fabrication of silicon nanowires by electron beam lithography and electrochemical size reduction", ***Nano letters,*** Vol. 5, No. 2, (2005), 275-280.
14. Han, H., Huang, Z. and Lee, W., "Metal-assisted chemical etching of silicon and nanotechnology applications", ***Nano Today,*** Vol. 9, No. 3, (2014), 271-304.
15. Geyer, N., et al., "Ag-mediated charge transport during metal-assisted chemical etching of silicon nanowires" ***ACS Applied Materials & Interfaces,*** Vol. 5, No. 10, (2013), 4302-4308.
16. Zeis, R., Lei, T., Sieradzki, K., Snyder, J. and Erlebacher, J., "Catalytic reduction of oxygen and hydrogen peroxide by nanoporous gold", ***Journal of Catalysis,*** Vol. 253, No. 1, (2008), 132-138.
17. Hildreth, O., Rykaczewski, K. and Wong, C.P. "Participation of focused ion beam implanted gallium ions in metal-assisted chemical etching of silicon", ***Journal of Vacuum Science and Technology B:Nanotechnology and Microelectronics,*** Vol. 30, No. 4, (2012), 040603.
18. Yue, Z., Shen, H., Jiang , Y., Wang, W. and Jin, J., "Novel and low reflective silicon surface fabricated by Ni-assisted electroless etching and coated with atomic layer deposited Al2O3 film", ***Applied Physics A,*** Vol. 114, No. 3, (2014), 813-817.
19. Bai, F., Li, M., Song, D., Yu, H., Jiang, B. and Li, Y., "One-step synthesis of lightly doped porous silicon nanowires in HF/$AgNO_3$/H_2O_2 solution at room temperature", ***Journal of Solid State Chemistry,*** Vol. 196, (2012), 596-600.
20. Divan, R., Rosenthal, D., Karim Ogando, K., Ocola, L.E., Rosenmann, D. and Moldovan, N., "Metal-assisted etching of silicon molds for electroforming", ***Journal of Vacuum Science & Technology B, Nanotechnology and Microelectronics: Materials, Processing, Measurement, and Phenomena,*** Vol. 31, No. 6, (2013), 06FF03.
21. Chang, S.W., Chuang, V.P., Boles, S.T., Ross, C.A. and Thompson, C.V., "Densely packed arrays of ultra-high-aspect-ratio silicon nanowires fabricated using block-copolymer lithography and metal-assisted etching", ***Advanced Functional Materials,*** Vol. 19, No. 15, (2009), 2495-2500.
22. Peng, K., Hu, J.J., Yan, Y.J., Wu, Y., Fang, H., Xu, Y., Lee, S.T. and Zhu, J., "Fabrication of single-crystalline silicon nanowires by scratching a silicon surface with catalytic metal particles", ***Advanced Functional Materials,*** Vol. 16, No. 3, (2006), 387-394.